



Assessment of Protective Effect of Rutin Utilizing Advanced Intranasal Nanoparticulate System in Mice Model after Experimental Challenge with *Pasteurella Multocida* Isolated from Naturally Infected Sheep

Iman A.M. Abdel-Rahman¹, Amany M. Mohamed², Nagwa I. Toaleb², Ahmad M. Allam², Sherein S. Abdelgayed^{3,4}, Abeer S. Hassan^{*5} and Sahar H.A. Hekal⁶

¹ Department of Pharmacognosy, Faculty of Pharmacy, South Valley University, Qena 83523, Egypt.

² Department of Parasitology and Animal Diseases, Veterinary Research Institute, National Research Centre, 33 Bohouth St., Dokki, 12622 Giza, Egypt.

³ Pathobiology department, College of Veterinary Medicine, Tuskegee University, AL36808, USA.

⁴ Department of Pathology, Faculty of Veterinary Medicine, Cairo University, 12211, Giza, Egypt.

⁵ Department of Pharmaceutics, Faculty of Pharmacy, South Valley University, Qena 83523, Egypt.

⁶ Department of Natural Resources Faculty of African Postgraduate Studies, Cairo University, Giza, Egypt.

Abstract

RUTIN is a promising nutraceutical with potential antibacterial and prophylactic activities. This work aimed to evaluate the protective effect of Rutin nanovehicle, which were formulated as a mucoadhesive intranasal preparation, on mice experimentally challenged with *Pasteurella multocida*. The extracted Rutin nanopatform was laden into different concentrations of mucoadhesive hydroxy propyl methyl cellulose (HPMC). The ex vivo permeability of Rutin nanoformulations across the nasal mucosa was evaluated. The optimal formulation was examined in vivo, and group 1 was not infected or prophylactic. Group 2 was infected with *P. multocida*-nonprotected, and groups 3 and 4 were prophylactic groups that were protected with free Rutin extract and Rutin nanoformulation, respectively, via the intranasal route. The bacterial count in vital organs was carried out post challenge with *P. multocida* to determine protective effect of free Rutin extract and Rutin nanoformulation, also pathological changes in the vital organs were examine, level of IgG was determined, Cytokines concentration; Interferon Gamma (INF- γ) and Interlukin-12 (IL -12) was assessment by using sandwich ELISA. The rutin nanoparticulate system containing the lowest amount of HPMC exhibited enhanced permeated amount ($311.64 \pm 10.0 \mu\text{g}/\text{cm}^2$) and steady state flux $6.67 \pm 0.10 \mu\text{g}/\text{cm}^2/\text{sec}$ across nasal mucosa. The results of the in vivo study revealed that the rutin nanoformulation showed a significant reduction in the bacterial count, histopathological lesions in the examined organs. Also, increased the hormonal response of mice where it increased levels of antibodies IgGs and modulation in the concentration of serum IFN- γ and IL-12. The mucoadhesive intranasal Rutin nanovehicle has remarkable immunomodulatory effects and can be used for protection against *Pasteurella multocida* in animals.

Keywords: *Pasteurella multocida*, prophylaxis, free Rutin extract, Rutin nanostructure lipid carrier.

Introduction

Globally, Pasteurellosis is widely diffused and can be distributed among both species and regions [1]. *P. multocida* is one of the normal microflora of the nasopharyngeal region. *P. multocida* colonised in this region for long periods without any clinical symptoms until animals subjected to stresses factor, like transportation for a long distance, overcrowding, decreased immunity of the host, and changes in surrounding humidity or temperature. Under the influence of these stressors, *P. multocida* proliferates and migrates from the upper respiratory tract to

invade the lower respiratory tract, resulting in pneumonia [1, 2].

Pasteurella was first mentioned by Perroncito in 1878. This bacterium was named after Louis Pasteur, who first recognised *P. multocida* as an agent responsible for fowl disease in 1880. It causes haemorrhagic septicaemia (H.S) in ungulates, snuffles in rabbits, fowl cholera in chickens, pneumonia, and atrophic rhinitis in pigs. Humans infected with *P. multocida* after biting from dogs or cats may develop pulmonary disease and soft tissue infections [3], but human deaths are uncommon [1].

*Corresponding Author: Abeer S. Hassan, E-mail: abeer.saad@svu.edu.eg, Tel.: +201012060262

ORCID: <https://orcid.org/0000-0001-8984-2957>

(Received 19 June 2024, accepted 14 November 2024)

DOI: 10.21608/EJVS.2024.297980.2183

©National Information and Documentation Center (NIDOC)

These diseases have a great economic impact around the world, where more than \$1 billion is lost annually to the beef cattle industry in North America alone [4].

Although antibiotics are the primary treatment for pasteurellosis in animals, they are not effective in treating acute to acute pasteurellosis such as haemorrhagic septicaemia. Additionally, this treatment strategy is expensive and lengthy and becomes ineffective due to increased drug resistance of the bacterium [5]. Immoderate antibiotic use can cause toxicity in humans [6]. Because of the emergence of antibiotic-resistant bacteria, there is a need to investigate effective antimicrobial agents or create innovative formulations for treating infections [7].

Rutin (RUT) is a glycosylated polyphenolic phytochemical that is widespread in coloured fruits and vegetables. Rutin is a natural flavonoid that belongs to the flavone family found in different plants, and its antibacterial efficacy has been studied in previous studies [8-10].

Nanoparticles have been utilised previously for the delivery of antibacterial and antifungal agents into the lungs [11], [12], validating drug release after pulmonary administration [13]. It can be formulated to achieve acceptable morphological characteristics in the form of powders for respiratory inhalation [14].

Nanomedicine has attracted immense interest in pharmaceutical research, offering promising designs for medical applications. Nanotechnology can provide precise medication for controlling various infections. Successful therapeutic application of nanocarriers for delivering herbal natural products could be related to modification of the physicochemical properties of encapsulated bioactive phytochemical products [15, 16]. Different nanovehicles have been reported to deliver active natural products such as polymeric, solid lipid nanoparticles, nanoemulsions, nanovesicles, and nanocrystals.

Nanostructured lipid carriers (NLCs) consisting of a solid and liquid lipid mixture, resulting in a matrix structure that provides sufficient space to encapsulate active product in the matrix. Therefore, NLCs have higher drug encapsulation efficiency (EE) and physical stability in storage for long-term in comparison with solid lipid nanoparticles (SLNs) [16, 17]. NLCs are all considered factors that can overcome the drawbacks of other colloidal carriers. Mostly, NLCs predominate polymeric nanoparticles (NPs) with safety and biocompatibility properties and are considered the least toxic NPs when administered to living tissues [17, 18].

Scientists have recently been exploring the use of natural products, such as bioflavonoids, in the healthcare system due to their wide range of biological activities and high safety margins. Rutin, a

polyphenolic natural compound, has shown various pharmacological activities due to its effective antioxidant characteristics [19].

Moreover, they explained the use of nanostructured lipid carriers (NLCs) for Ciprofloxacin (CIP) to increase the deposition and accumulation into deeper tissues of the lungs for the management of non-cystic fibrosis bronchiectasis (NCFB) [20]. In addition, Patil and Jobanputra [21] reported that the antibacterial efficacy of rutin was significantly improved by formulating it as rutin-loaded chitosan nanoparticles.

In our laboratory, we reported that intranasal treatment using the natural product of Rutin loaded in nanostructure lipid carriers, which have potential antibacterial effects against *P. multocida* infection, and the treatment with RUT- NLCs showed the highest effect against *P. multocida* infection [22]. Additionally, in our previous laboratory study, the results revealed that the optimum Rutin-NLC formulation was smaller in particle size and superior in encapsulation and antibacterial activity when compared with the Rutin niosome formulation.

In this study, we investigated for the first time the prophylactic effect against *P. multocida* of extracted natural rutin using an advanced mucoadhesive nanoparticle; we used the same components of an NLC formulation that was selected in our previous study [22]. The developed Rutin-NLCs were then expressed as an intranasal mucoadhesive formulation via mixing with different concentrations of hydroxypropyl methyl cellulose (HPMC as mucoadhesive polymer). Mucoadhesive formulations were characterised for *ex vivo* permeation across the nasal mucosa, and the optimal formulation was evaluated as a prophylactic agent *in vivo* in an infected mice model. The prophylactic effect of a mucoadhesive Rutin nanostructure lipid carrier compared with free extracted Rutin was evaluated when administered as an intranasal delivery system to protect mice as a model from infection with *P. multocida*.

Material and Methods

Ethics Statement

This study was carried out in accordance with the guidelines of the institutional Animal Care (Committee at Faculty of Pharmacy -South Valley University) (approval no. P.S.V.U 144/22)

Sample Collection

Nasal swabs were collected from infected sheep in a private farm in Giza province, where the infected animals suffered from fever with respiratory manifestations, including difficult breathing, dyspnoea, coughing, and nasal discharge. A total of 25 samples were collected from the nasal cavity of infected sheep using sterile cotton nasal swabs after

cleaning the nasal area with 70% alcohol. Samples were quickly transferred to the laboratory in ice boxes, and all samples were placed in nutrient broth and incubated at 37° C for 24 h.

Bacterial Isolation

Samples were cultured on blood agar containing 5% sheep blood and MacConkey agar and incubated at 37° C for 24 h. Isolate identification followed conventional bacteriological techniques, including colony morphological assessment on culture media, Gram staining, microscopic feature examination, and biochemical testing.

Biochemical Tests

All the isolates were tested biochemically by sugar fermentation tests by growing the suspected *P. multocida* isolates in Peptone water, inoculated in 1% glucose, mannitol, sucrose, lactose, arabinose, trehalose, and mannose, and incubated aerobically at 37°C for 72 hours. Indole, oxidase, catalase, urease production, triple sugar iron agar (TSI), methyl red (MR), Voges-Proskauer test (VP), and nitrate reduction tests were carried out according to their standard bacteriological procedure [23].

Pathogenicity Test

Nine Swiss albino male 5-week-old mice were used for pathogenicity testing, two mice each for suspected *P. multocida* isolates and one mouse was used as a control. Each mouse was inoculated intraperitoneally with 0.1 ml of inoculum containing 0.3×10^8 organisms per ml in sterile normal saline. The control mice were inoculated with 0.1 mL of sterile saline. All mice were observed, and mortality was recorded. Blood smears were prepared from the heart blood of dead mice and stained with Leishman's stain. Re-isolation of *Pasteurella* from the heart blood of the dead mice occurred on 5% sheep blood agar and was identified biochemically.

Animals

Sixty healthy Swiss albino male mice with an age range from 4-5 weeks (each mouse weight 20–25 gm.) were obtained from the Animal house at National Research Centre, Dokki Giza, Egypt. Each group was housed in individual cages and kept in good hygienic conditions at room temperature of (25±3) with a 12 h dark/light cycle. They were fed with standard laboratory feed and watered, and after 7 days of acclimation, the experiment was started [24].

Bacterial Inoculum Preparation

Bacterial colonies isolated from the heart blood of mice were cultured in brain heart infusion (BHI) broth and incubated at 37°C overnight. Subsequently, the bacteria were sub-cultured for 3 h in a shaking incubator at the same temperature. After washing the bacterial cells twice, they were re-suspended in sterile phosphate-buffered saline (PBS). The

bacterial density was determined using McFarland standards, and an inoculum containing 10^8 colony-forming units (CFU) per millilitre was prepared. The CFU/ml count was calculated using the spread-plate method on a BHI agar plate [25].

Plant Material

Fresh flowers of *Matricaria chamomilla* were collected from a cultivated area near South Valley University. A voucher specimen of the plant (code: Gc.78) was kept in the herbarium of the Department of Pharmacognosy, Faculty of Pharmacy, South Valley University, Egypt. The collected fresh flowers were washed with tap water to remove any associated particles. The plants were placed at room temperature to dry before being ground into a fine powder.

Chemicals

Surfactant (Tween 80) and lipids (stearic acid, and oleic acid) were purchased from Alpha Chemicals Co., Cairo, Egypt. Hydroxy propyl methyl cellulose (HPMC15,000) was donated by El Gomhouria Co., Cairo, Egypt.

Extraction of Rutin Samples

In this work, pure rutin was obtained via extraction according to a previously mentioned method with slight modification [26]. In brief, 200 g of ground dried *Matricaria chamomilla* flowers were weighed into a glass bottle, and 15 mL of a hydroalcoholic solution composed of 74% water and 26% ethanol was added. The tube was tightly closed and agitated in a hot water bath at a temperature of 60 °C at 200 rpm for 30 min. The extract was filtered and fractionated to obtain pure rutin, as presented in the supplementary material. Its identity was confirmed by ^1H and ^{13}C NMR.

Preparation of Rutin-loaded Lipid Carriers

The extracted rutin was loaded into NLCs using emulsification and solvent evaporation accompanied by ultrasonication according to previous used method in our laboratory [22]. The total lipid mixture (1000 mg) consisted of liquid lipid (oleic acid 500mg) and solid lipid (stearic acid, 500 mg) were dissolved in organic solvent at a 70°C at ratio of (1:1) to prepare the lipid phase. The aqueous phase was generated using preheated distilled water (20 mL) consisting of Tween80. Then, the aqueous phase was added slowly to the lipid phase, and the mixture was stirred on a magnetic stirrer at 2000 rpm were mixed for 2 h to evaporate the organic solvents. The resultant dispersion was sonicated for 10 min using probe sonication (Acculab, UP850, USA) at pulse-ON for 3 s and pulse-OFF for 3 s. Different concentrations of HPMC (0.1, 0.25, 0.5 and 0.75 %w/v) were added to the developed dispersion of RUT-NLCs (20 ml) to produce slightly viscous mucoadhesive nanodispersions of RUT-NLCs (Table 1). The

developed mucoadhesive formulation was kept at room temperature on a magnetic stirrer at 1000 rpm for 1 h to be stabilised and finally placed at 4°C overnight for further studies.

The developed intranasal Mucoadhesive formulations containing RUT-NLCs were evaluated for appearance, pH, and viscosity. The viscosity of the developed preparations was measured using a Brookfield digital viscometer (DV-II, Brookfield Engineering Laboratories, Stoughton, MA) at 25°C using a spindle number of 96 at a shear rate of 15 rpm. The experiments were performed in triplicate.

Ex vivo Intranasal Permeation Study

Ex vivo permeation studies were conducted for different RUT-HPMC-NLCs formulations and compared with free extracted RUT suspensions using sheep nasal mucosa according to previous procedures [27]. The nasal mucosa was washed with distilled water. Then the mucosa was cleaned with simulated nasal fluid SNF (pH 5.5). Mucosal tissues were placed over one end of open-ended glass tubes with a surface area of 1.57 cm². The examined Rutin formulations (calculated volume of free RUT suspension or RUT-HPMC- NLC formulations corresponding to 0.5 mg of RUT) were fixed over the nasal mucosa. The glass tubes were immersed in a glass beaker containing 50 mL of SNF (pH 5.5 with 0.25%, v/v ethanol). The beakers were agitated at 50 r.p.m and 37 ± 0.5 °C for 24 h using a shaking water bath, (DAIHAN Scientific Co., Seoul, South Korea). At different time points (0.5, 1, 2, 4, 6, 12, and 24 h), samples of 3.0 mL were removed, replaced with an equal volume of fresh SNF medium to maintain the sink condition. Samples were analysed for RUT content using a UV spectrophotometer at a maximum wavelength of 359 nm. The determinations were performed in triplicate. The cumulative amount of permeated drug was plotted versus time. The slope of the linear part in the line was calculated as the steady state flux (J_{ss}) The apparent permeability coefficient (P_{app}) was estimated using the following equations[28].

$$P_{app} = J_{ss}/C_0$$

Here, P_{app} is the apparent permeability coefficient (cm/h), J_{ss} is the steady-state flux (mg/cm².h), and C₀ is the initial drug concentration in the donor compartment (mg/ml).

The data are presented as the mean of three measurements ± SD.

Experimental Design and Protection Protocol

Sixty healthy male mice were divided randomly into four equal groups (15 per group). The first group (group1) was kept as the normal control negative group (uninfected- non prophylactic) in which each mouse received 50 µL sterile PBS intranasally 2 times/week for 2 weeks and after two weeks injected

with sterile PBS 100 µL / mouse intraperitoneal. The second group (group2) was considered the infected group with *P. multocida* (infected-non protected) each mouse received 50 µL sterile PBS intranasal 2 times/week for 2 weeks. Two weeks later, mice were infected with one shot via intraperitoneal injection with sterile PBS 100 µL / mouse of the bacterial cell suspension matching a 0.5 McFarland standard solution (1.5×10⁸cfu). Group three and four (group 3 & 4) were considered prophylactic groups in which mice were injected intranasally with free Rutin extract (5 mg/kg) and mucoadhesive nanostructure lipid carriers (RUT-NLCs) containing 0.1 % w/v HPMC (F1) (5 mg/kg), respectively 2 times/week for 2 weeks and after 2 weeks of challenge with *P. multocida* intraperitoneal injection with sterile PBS 100 µL / mouse of the bacterial cell suspension matching a 0.5 McFarland standard solution (1.5×10⁸cfu). Mice in all groups were maintained in an upright position for 30 s after intranasal inoculation to maintain the drug localised in the nasal cavity for an extended period [29]. All mice in the groups were checked daily for any changes for 1 week post infection.

Blood sampling and vital organs

Blood samples were collected at zero days, one, two, and three weeks after challenge from the mice of all groups via the medial canthus of the eyes of the mice. Sera were separated and frozen at -20°C for further use for assessment of Interferon Gamma (INF-γ) and Interlukin-12 (IL -12) serum levels.

Three mice from each group were sacrificed after anaesthesia at 24, 48, and 7 days post challenge with *P. multocida* to determine the bacterial count (CFU/g of tissue) in vital organs (lung, liver and spleen) of mice and examine histopathological changes.

Bacterial Colonisation/count

Three mice from each group were sacrificed after anaesthesia at 24, 48, and 7 days post challenge with *P. multocida* to determine the bacterial count (CFU/g of tissue) in vital organs (lung, liver and spleen). From each organ (lung, liver and spleen), 0.1 g was collected. The tissues were homogenised aseptically and bacterial loads were quantified by 10-fold serial dilution in saline. These different dilutions were plated in triplicate in blood agar and were incubated at 37°C up to 24 h to count CFU/g.[29]

Preparation of the specific Pasteurella multocida

Antigen

The antigen of *P. multocida* (PM antigen) was prepared from the homogenate of the isolated strain in 0.15 M PBS (PH 7.2) after repeated freezing and thawing of isolates to rupture the bacterial wall. The samples were then sonicated in ice and centrifuged at 14,000 rpm for 30 min at 4°C. The protein content of

the antigen (*P. multocida* antigen) was determined by Lowry *et al.*[30].

Serum Cytokine Level Analysis

Cytokines levels INF- γ and IL -12 were determined using a commercial ELISA kit (Sunlong Biotech Co., Ltd., China) according to the procedures recommended by the manufacturer's instructions.

Enzyme Linked Immunosorbent Assay (ELISA)

Indirect ELISA was adopted to evaluate the protective IgG levels due to pure Rutin and Rutin mucoadhesive Nanostructure lipid carriers (F1) (RUT-NLCs) formulations compared with the control group in mice serum samples collected at different week intervals of infection according to Engvall and Perlmann [31]. The plates were separately coated with 40 μ g /ml PM antigen in carbonate buffer. The optimum antigen concentration, antibody, and conjugate dilutions were determined by checkerboard titration. An anti-mouse IgG horse radish peroxidase conjugate and an ortho-phenylenediamine (OPD) substrate buffer (Sigma) were used. The cut off values of optical density (OD) were calculated as described by Hillyer *et al.*[32]

Histopathological Examination

Liver, lung, and spleen samples were obtained from various experimental groups and underwent routine processing. Paraffin-embedded blocks were cut into 5-micron-thick sections and stained with Haematoxylin and Eosin [33] for histopathological examination using a light microscope (Olympus BX50, Japan).

Grading of Histopathological Alterations

Histopathological alterations in the liver, lungs, and spleen were graded as (0), no changes; (+), (++) , and (+++) indicated mild, moderate, and severe changes, respectively [34].

Statistical Analysis

The statistical analysis was performed using SPSS 19.0 for Windows (SPSS, Inc., USA). Data are expressed as means and standard errors. Descriptive analysis, One-way Anova, and post hoc (Duncan) tests were carried out for intergroup comparisons. $P < 0.05$ were interpreted as statistically significant [35].

Results

The optimum rutin-loaded NLC formulation (RUT-NLCs) was selected based on the obtained results in our research study [22] was successfully formulated and then mixed with different concentrations of HPMC (0.1, 0.25, 0.5 and 0.75 %w/v) to prepare mucoadhesive intranasal NLC dispersions (Table 1). In the present study, we investigated the improved prophylactic biological

performance of Rutin when delivered as a mucoadhesive intranasal HPMC-NLC compared with a pure rutin suspension. The developed RUT-NLCs had a small particle size with a small value of P.D.I. and high drug encapsulation (the results were presented in previous our study) [22]. Different concentrations of HPMC influenced the properties of the prepared mucoadhesive RUT-NLC formulations, and the results are presented in Table 1. All formulations were homogenous in appearance and had appropriate pH values for nasal applications. Further, F1, which contained the lowest concentration (0.1 %) of HPMC exhibited lowest viscosity compared with other formulations.

Ex vivo Intranasal Permeation Study

The cumulative amount of Rutin from the examined formulations that permeated across the nasal membrane was evaluated, and the results are illustrated in Figure 2 and Table 2. Figure 2 shows that the amount permeated from all examined mucoadhesive RUT-HPMC-NLC formulations across fresh nasal mucosa was significantly higher ($p < 0.001$) than that from the free extracted Rutin suspension. Formula F1 showed a higher significant permeation amount than the other formulations. The permeability coefficient was estimated and found to be of 1.85 ± 0.005 , 1.40 ± 0.009 , 1.18 ± 0.003 and $0.846 \pm 0.001 \times 10^{-6}$ (cm/sec) for mucoadhesive RUT-HPMC-NLCs formulations (F1, F2, F3 and F4, respectively) and $0.55 \pm 0.002 \times 10^{-6}$ cm/s for the pure RUT suspension after 24 h (Table 2). The F1 formulation exhibited superior enhancement (3.37-folds) of permeation across the nasal mucosa compared with free pure Rutin. Based on the results of the *ex vivo* permeation study, mucoadhesive nanoformulation F1, which consists of 0.1 % w/v of HPMC mixed with the rutin nanosystem (RUT-NLC), was selected for *in vivo* prophylactic study in a mouse model.

Bacteriological Characterisation

Out of 25 samples, 4 isolates (16 %) were identified as *P. multocida*. The isolates of *P. multocida* grew on blood agar without haemolytic effect and did not grow on MacConkey agar, Gram stained explained that these bacterial isolates were Gramme negative short rods or coccobacilli. The isolates were identified biochemically, and the results are presented in Table (3)

Pathogenicity Test

Upon reisolation from the lung, the isolate exhibited typical morphological and cultural features, including dewdrop-like, mucoid, non-haemolytic colonies on blood agar. Additionally, culture smears revealed characteristic Gram-negative coccobacilli, whereas impression smears from heart blood demonstrated bipolarity upon Leishman staining, as depicted in Fig.(3).

In vivo Study Results

Clinical symptoms and mortality rates

No clinical signs were observed in the control group, and no deaths occurred during the experiment. While the infected group showed clinical symptoms such as depression, loss of appetite, nasal discharge, and fever in the first 24 h, two mice died after 24 h pi, the mortality rate was 13.33% at first 24 h pi, followed by another five mice died at 36 h pi (the mortality rate was 33.33%) from the infected group before death, they showed severe difficult respiration and increased nasal discharge, finally the last 8 mice showed severe dyspnoea and died at 48 h, the mortality rate reached to peaked at 53.33% at 48 h pi. While group3 protected with free RUT also showed depression, loss of appetite, and nasal discharge, two mice were dead at first 24 h post challenge in ratio (13.3%) and after 24 h pi the symptoms decline until it disappeared with no more mortality occurring. Group 4 showed the same symptoms as group 3 at the first 24 h post challenge and after 48, the symptoms disappeared; however, in this group, no mortality occurred, and the survival rate was (100%).

P. multocida counts in mouse organs

An *in vivo* study was carried out to estimate the effects of free RUT and mucoadhesive RUT-HPMC-NLCs in mice experimentally infected with *P. multocida*. The bacterial counts of vital organs such as the lung (Table 4 a), liver (Table 4 b), and spleen (Table 4 c) homogenates of different groups were measured. *P. multocida* was not detected in the lung, liver, and spleen of mice of group 1 (normal control negative). *P. multocida* was detected in all tissues of the infected group (group2) at 1 and 2 dpi. The bacterial contents in the lung, liver, and spleen of the infected group were relatively low at 1 dpi, then bacterial count at 2 dpi of the same group; bacterial load in the lung and liver were similar to those in the spleen, peaking at 2 dpi. The spleen had the highest number of *P. multocida* than the bacterial count in the lung and liver of the same group, where the average number of *p. multocida* in the spleen at 24 h and at 48h was $1.74 \pm 0.112 (\times 10^8)$ and $2.11 \pm 1.46 (\times 10^9)$ CFU/g, respectively. The average numbers of *P. multocida* in the lung and liver of the infected group at 24h and 48h was $2.4 \pm 0.12 (\times 10^7)$ and $2.8 \pm 0.12 (\times 10^8)$ CFU/g respectively in lung and $2.16 \pm 0.07 (\times 10^5)$ and $2.38 \pm 0.161 (\times 10^6)$ CFU/g in the liver. The average numbers of *P. multocida* in the lung, liver, and spleen of mice in group3 (protected with free RUT) at 24 h, 48 h, and 7 days post challenge with *P. multocida* was $1.74 \pm 0.1 (\times 10^6)$, $2.56 \pm 0.09 (\times 10^5)$ and $5 \pm 2.64 (\times 10^2)$ in the lung, $2.12 \pm 0.27 (\times 10^4)$, $1.13 \pm 0.11 (\times 10^3)$ and $2.33 \pm 1.52 (\times 10^2)$ in the liver, $5.76 \pm 1.8 (\times 10^7)$, $1.59 \pm 0.16 (\times 10^5)$ and $2.33 \pm 1.5 (\times 10^2)$ in the spleen. The average number of *P. multocida* in the lung, liver, and spleen of mice in

group 4 (protected with RUT-HPMC- NLCs selected formulation) at 24 h and 48 h post challenge with *P. multocida* was $2.45 \pm 0.19 (\times 10^5)$, $1.96 \pm 0.1 (\times 10^3)$ in the lung, $1.14 \pm 0.13 (\times 10^4)$, $1.96 \pm 0.1 (\times 10^3)$ in the liver, $2.45 \pm 0.10 (\times 10^5)$, $2.34 \pm 0.12 (\times 10^3)$ in the spleen. *P. multocida* was not detected in the lung, liver, and spleen of mice in the group protected with RUT-HPMC- NLCs at 7 days post challenge with *p. multocida*. From the previous result, we noticed a decline in the average number of *p. multocida* in group3 and in group4 from 24 h to 48 h, 7 days until it disappears at 7 days post infection in group protected with RUT-HPMC-NLCs. There was a significant difference between tested groups (3 and 4) compared with infected group (2) (at $p < 0.05$). Also, there was a significant difference between the group that treated with RUT-HPMC-NLCs selected formulation compared with that treated with RUT. (At $p < 0.05$). The counts of bacteria in the lungs, liver, and spleen in different groups of mice at 24, 48, and 7 dpi. Represented as means \pm SD in Table 4 (a, b, and c).

Protective Humoral Immune Response

The IgG levels in mice in the protective groups were higher than those in the control group Figure (3). The IgG level in mice intranasally inoculated with mucoadhesive Rutin nanostructure lipid carriers (RUT-HPMC-NLCs) (group 4) and challenged with *P. multocida* bacterial suspension was the highest IgG level with *P*- values < 0.001 high statistical significance than in mice intranasally inoculation with Free Rutin (group3) and challenged with the same concentration of *P. multocida* suspension. The IgG levels against the two extracts (RUT-HPMC-NLCs and Free Rutin) increased gradually after the first booster (0.923 ± 0.005 and 0.613 ± 0.001 , respectively) until the date of challenge (on the second week) with the *P. multocida* bacterial suspension (1.02 ± 0.005 and 0.693 ± 0.007 , respectively). The mucoadhesive formulation RUT-NLCs had the highest potency among the others starting from the first week post intranasally inoculation, and the enhanced immune response reached a maximum (1.156 ± 0.007) at the third week post protection, which represented the first week of challenge with *P. multocida* (Figure (4)). The average of OD values was summarised in Table 5.

Cellular Immune Response

The concentration Levels of IFN- γ were significantly higher in the protected two groups; group 4 (protected with RUT-HPMC-NLCs) and group 3 (protected with Free RUT), than in the non-protected infected group and normal group. Throughout the experiment, the rutin nanostructure lipid carrier (RUT-HPMC-NLCs) was high statistical significance *P*- values < 0.001 , recording the highest value (440 ± 2.89) three weeks post protection and one week post challenge (Table 6). Concentration

values of IL-12 were also significant higher P- values < 0.05 in mice group 4, which were intranasally inoculated with Rutin nanostructure lipid carriers (RUT-HPMC-NLCs) at week three post protection and one week post challenge (240.17±1.71) than the other extract Free Rutin post challenge and healthy, infected nonprotected groups. A significantly higher level of IFN- γ than IL- 12 was observed throughout the experiment (Table 6).

Histopathological Findings

Liver: In the control group, the liver exhibited normal hepatic parenchyma characterised by polygonal hepatic cells, intact blood sinusoids, central veins, and well-defined portal areas (Fig. 5 (I), a), whereas liver from the control group exhibited severely degenerated hepatic parenchyma with mononuclear cell infiltration (Fig. 5 (I), b). Livers from mice of group 3 and group 4 who received free Rutin + PM and (RUT-HPMC-NLCs) Rutin nanostructure lipid carrier + PM groups exhibited variations of lesions improvement than the control positive group, including severe lesions regression in the liver of group 4 (protected with RUT-NLCs) with apparently healthy hepatic parenchyma (0) (Fig. 5, (I) c), and moderate improvement in the liver of group 3 (received free Rutin + PM) with congested hepatportal blood vessels and leucocytic cell infiltration (Fig. 5 (I), d).

Lungs: In the control group, the lung parenchyma exhibited typical bronchioles and alveoli, both of which were within normal parameters (Fig. 5 (II), a), whereas the lungs of the control group showed severe bronchitis with severe inflammatory reaction (Fig. 5 (II), b). Lungs from the protected group with RUT-NLCs showed variations of lesion improvement compared with the control positive group, including severe lesion regression in the lung of group 4 with apparently healthy lung parenchyma (Fig. 5 (II), c), and moderate improvement in the lung of group 4 with Moderate lesions of interstitial mononuclear cell infiltration (Fig. 5 (II), d).

Spleen: The spleen from the control group showed normal splenic parenchyma with normal white and red bulbs (Fig. 5 (III), a), whereas the spleen from the control group showed severely congested red bulbs and interstitial blood vessels (Fig. 5 (III), b). Spleen from the protected group with RUT-NLCs showed variations of lesion improvement compared with the control positive group, including severe lesion regression in group 4 with apparently healthy splenic parenchyma (Fig. 5 (III), c), and moderate improvement in the spleen of group 3 with moderately congested red bulbs and interstitial blood vessels (Fig. 5 (III), d).

Histopathological Lesion Scoring

All recorded lesions in the liver, lungs, and spleen were scored as shown in Table 7.

Discussion

The endeavour to develop drug delivery systems that overcome first-pass metabolism and based on intestinal degradation studies, we have determined that nasal administration meets these criteria and can be employed for drugs with the mentioned limitations. Therefore, in this investigation, intranasal RUT-NLC formulations containing different concentrations of HPMC as the mucoadhesive polymer were developed and evaluated (Table 1). The best mucoadhesive formulation with enhanced permeation across nasal tissue was selected to enhance the biological activity of Rutin in the prophylaxis against *P. multocida*. Mouse models of *P. multocida* serotype A infection provide a well-established experimental model for investigating immunopathological responses to infection. Rutin (Figure 1) is commonly used as a self-prescribed remedy for upper respiratory tract infections, including those caused by *Aeromonas hydrophila* [7]. The utilised nanopatform of Rutin (RUT-NLCs) was selected in this investigation according to previous work in our laboratory because of its small particle size diameter in the nanosized range [22], which is considered appropriate for nasal and pulmonary localisation. HPMC is a water-soluble polymer with efficient mucoadhesive properties in intranasal formulations. Therefore, the use of HPMC with RUT-NLC formulation provided mucoadhesive properties for a long time when applied to the nasal mucosa, which could offer a prophylactic against bacterial infection for a prolonged period. The mucoadhesive time for HPMC-NLC formulations in this study was significantly longer than that (Alginate-NLCs) obtained in our previous work[22]. The explanation of this result may be related to the nature of the mucoadhesive polymers HPMC is neutral and contains a neumerous hydroxyl group that allows the interaction of the formulation with the mucus and is attracted to mucosal tissue by hydrogen and van der Waals bonds [36]. Thus, mucoadhesive HPMC retained the drug-loaded NLCs and prolonged its contact time at the absorption site (nasal tissue). Sodium alginate is negatively charged at physiological pH, resulting in weak interaction with mucosal tissue because of electrical repulsion[37]. In addition, the selected concentration of HPMC (F1) (0.1%) showed suitable low viscosity that permitted rapid drug release from the nanocarrier formulation, achieving higher rutin nasal absorption. This low-viscosity dispersion may offer an advantage in the rapid release of drugs and improved nasal permeation, thus enhancing biological effects. Thus, HPMC at low concentrations offers an effective mucoadhesive intranasal delivery system for rutin NLCs. These results match those of a previous study [37].

Ex vivo permeation study across the nasal tissue was carried out for RUT-HPMC-NLC formulations

compared with free drug suspensions. The nasal cavity anatomy in sheep resembles that of humans, suggesting a correlation between *in vitro* and *in vivo* studies. Fig. 2 exhibits the cumulative drug amount permeated across the nasal mucosa from RUT-HPMC-NLC formulations and free Rutin. The results showed that the permeation was substantially enhanced using RUT-HPMC-NLCs compared with free Rutin. The enhanced permeability may be due to the high drug encapsulation of rutin and the small particle size of the developed nanosystem formulation. It has been reported that small particle sizes improve the transmucosal permeation of nanoparticulate systems [38]. Furthermore, the enhanced permeability may be due to the presence of oleic acid and a surfactant (Tween 80) in the formulation (NLCs), which helps in solubilisation. Hence, improved permeation could be attributed to the transcellular uptake, high solubilisation tendency, as well as the potential for boosted absorption. Moreover, the presence of neutral, low-viscosity HPMC (0.1% w/v, F1) as a mucoadhesive polymer mixed with Rutin nanocarrier (RUT-NLC) resulted in rapid drug release compared with other formulations containing higher amounts of HPMC polymer. Whereas permit the localisation of the high concentration of drug for long time at the absorption site (nasal tissue) and enhanced permeation of drugs into the nasal mucosa (Table 2). These results may be attributed to the strong mucoadhesive properties of HPMC, which provide attraction forces to the mucosal tissue, resulting in increased paracellular diffusion by limiting tight junctions. This mucoadhesive property can increase drug localisation at the application site, resulting in fewer administration times and doses and improving patient compliance. This result is similar to a previous study [39].

In describing the *in vivo* antibacterial and immunomodulatory effects of free Rutin and Rutin nanostructure lipid carriers (RUT-HPMC-NLCs), a mouse model of live *P. multocida* infection was used in the present study. In this model, the bacterial counts in the lung, liver, and spleen, histopathological lesions, and serum IFN- γ and IL-12 levels were studied.

P. multocida was spotted in all organs of the infected group, which was in accordance with Rezaie *et al.* [29] and yang *et al.* [1], which suggested that *P. multocida* can expeditiously imbue the host and reach various tissues and organs of mice, causing tissue damage and bacteraemia ended by death. In addition, from our results, the proliferation of *P. multocida* in tested tissues reached a maximum level at 2 dpi and had the highest mortality at the same time, which was consistent with the pathological findings recorded by Yang *et al.* [1]

Clinical observation of mice in group 4 protected with (RUT-HPMC-NLCs) demonstrated reliable conditions in parallel with those in the *P. multocida*-

infected group (group2). Besides, the bacterial count of group 4 protected with RUT-HPMC-NLCs showed significant variations with that of the *P. multocida*-infected group2 ($P < 0.05$). This result was confirmed by histopathological observations in group 4 (protected with RUT-HPMC-NLCs), which showed a nearly normal appearance, whereas group 3 (protected with free rutin) showed fewer lesions in comparison to the *P. multocida*-infected group (group2).

In this study, histopathological examination of the group infected with *P. multocida* at 48 h revealed different lesions in the targeted organs. The main changes in the lungs of the control group showed severe bronchitis with severe inflammatory reaction. These results agree with those of other earlier studies [29, 40, 41], which showed acute bronchopneumonia. Yang *et al.* [1] also found that *P. multocida* infection in rabbits initiated pathological lung damage. No evident pathological alterations were observed in the lungs of the control and prophylactic groups with mucoadhesive RUT-NLCs. In the free RUT-protected group, moderate interstitial mononuclear cell infiltration was observed. In the control group, the liver exhibited severely degenerated hepatic parenchyma with infiltration of mononuclear cells. Rezaie *et al.*, [29] recorded cell swelling in the livers of infected animals with *P. multocida* and diffuse neutrophil infiltration in sinusoidal spaces. In addition, blood vessels were engorged with red and white blood cells. The spleen of the control group showing severely congested red bulbs and interstitial blood vessel. While the prophylactic group with RUT-NLCs showed nearly normal spleen, the group protected with free RUT showed few lesions. Rezaie *et al.* [29] also showed the accumulation of neutrophils in the marginal zone of the white pulp in the infected group.

These findings indicated that the enhancement may be due to the bactericidal or immunomodulatory effects of the rutin mucoadhesive nanostructure lipid carrier (RUT-NLCs) and Free Rutin extract, a finding that is in agreement with previous reports [7, 13, 22, 42, 43]

While most studies have focused on the anti-inflammatory and antioxidant properties of rutin, limited research has been available on its immunomodulatory effects and underlying mechanisms. Interestingly, investigations have revealed that rutin exhibits a bidirectional immune regulatory effect. Not only does it play an immunosuppressive role by modulating cytokines and immune-related pathways, but it also enhances immune function. Rutin increases antibody levels, elevate immunoglobulin levels, and restore leucocyte function in treated rats, including by enhancing the phagocytic index [44]. In this study, we found that the animals that received RUT-NLCs had higher IgG

levels than the other groups starting from the first week post intranasally inoculation and still enhanced the humeral immune response. This result proved that RUT-NLCs have an immunoenhancing role in *P. multocida* infection and increase the IgG antibodies for protection.

Rutin and curcumin can play a role in reducing inflammation and decreasing lipid levels [45, 46] through the regulation of signalling pathways. Therefore, in this study, we found that the level of serum IFN- γ concentration showed significant differences $P < 0.001$ between the PM-infected group, healthy control group, protected with RUT-HPMC-NLCs, and group protected with free RUT. Also, concentration values of IL-12 showed higher significant P - values < 0.05 in mice group 4, which were intranasally inoculated with mucoadhesive Rutin mucoadhesive nanostructure lipid carrier (RUT-HPMC-NLCs) at week three post protection and one week post challenge (240.17 ± 1.71) but this value was less than infected nonprotected group 2. These data indicate that bacterial inoculation can increase cytokine levels, followed by inflammatory reactions. Like the present study, [47, 48] reported higher who reported strong Th1 immune responses in mice throughout *P. multocida* infection. IL-12 has a valuable regulatory role in Th1 responses by inducing the differentiation of naïve CD4 cells into Th1 cells and activating natural killer cells to produce IFN- γ . Also, our results agreed with Nguyen *et al* [49] who testified that IFN- γ activates both neutrophils and macrophages for intracellular killing of bacteria.

Conclusion

In conclusion, the extracted rutin was mixed with HPMC to develop a mucoadhesive intranasal preparation. The selected formulation containing 0.1% HPMC was examined for intranasal biological effects (in-vivo prophylactic action). The permeability of rutin in the mucoadhesive HPMC-NLCs formulation was significantly higher than that of the free rutin suspension. Intranasal administration of mucoadhesive nanostructure lipid carriers loaded with Rutin (RUT-HPMC-NLCs) for 2 weeks before the induction of pneumonia by *P. multocida* prevented bacterial growth in the lung, liver, and spleen, consequently reducing histopathologic lesions in these organs and modulated the concentration of serum IFN- γ and IL-12 concentrations in challenged mice. Thus, the mucoadhesive intranasal suspension of RUT-NLCs can be used as a natural nanoherbal drug to prevent and control pneumonia caused by *P. multocida*. Considering the widespread bactericidal, immunomodulatory, and anti-inflammatory properties of pure Rutin, this scenario increased the potential of utilising the examined mucoadhesive nanocarriers to enhance RUT permeability across the

nasal mucosa and increase drug residence time in the nasal tissue, possibly increasing its nasal absorption. Consequently, the biological effects are improved in tested animals. Thus, a mucoadhesive nanostructure lipid carrier formulation loaded with Rutin could be a valuable nano-nutraceutical intranasal drug delivery system for respiratory bacterial infection. Thus, Nanomedicines have attracted considerable attention for their efficient and safe drug delivery. In addition, it provides a new opportunity to develop intranasal vaccines and drug delivery systems for bacterial infections.

Acknowledgement

The authors are thankful to the National Research Centre veterinary institute and Institutional Animal Ethical Committee Institutional Animal Care and Use Committee at the Faculty of Pharmacy, South Valley University for permitting us to conduct the study.

Data Availability Statement

All data generated or analysed during this study are included in this published article and its supplementary files.

Competing Interests

The authors declare no conflicts of interest.

Funding statement

This research did not receive any specific grant from funding agencies in the public, commercial, or not-for-profit sectors.

Ethics statement

This study was performed in accordance with the guidelines set forth by the Animal Care and Use Committee of the Faculty of Pharmacy, South Valley University. The experimental protocol was approved by the Research Ethics Committee and the head of the Pharmacology and Toxicology Department (Approval No. P.S.V.U 144/22).

Conflicts of Interest

The authors declare no conflicts of interest.

Author Contributions

All authors contributed to the study conception and design. Material preparation, data collection, and analysis were performed by Abeer S. Hassan, Nagwa I. Toaleb, Ahmad Mohammad Allam, Amany M. Mohamed, Sherein S. Abdelgayed, Iman AM Abdel Rahman, and Sahar Hussein Abdalla Hekal. The first draft of the manuscript was written by Abeer. Hassan, Amany M. Mohamed, Nagwa I. Toaleb, and all authors have commented on previous versions of the manuscript. All authors have read and approved the final manuscript.

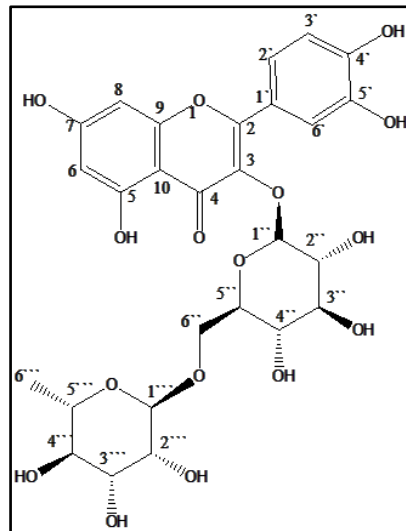


Fig. 1. Chemical structure of the extracted rutin

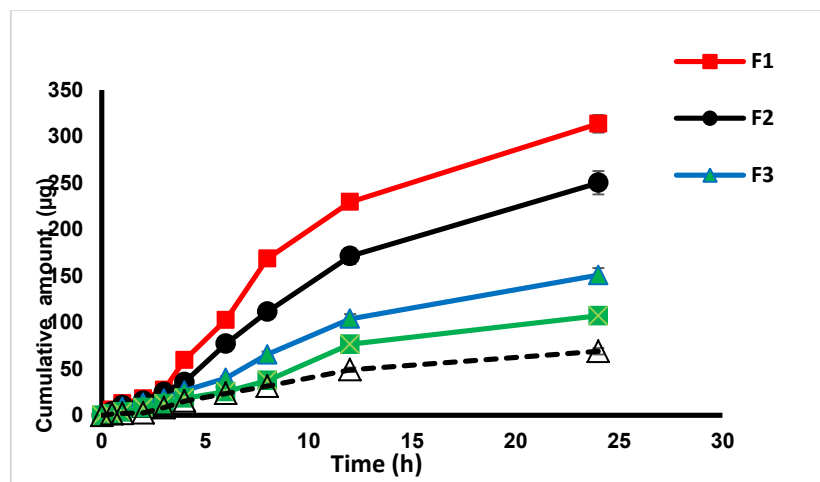


Fig. 2. *Ex-vivo* permeation profiles through nasal mucosa of RUT-HPMC-NLCs formulations compared with free RUT suspension in the simulated nasal fluid (SNF) (pH 5.5 for 24 h at 37 °C). Data were presented as mean \pm SD (n = 3)

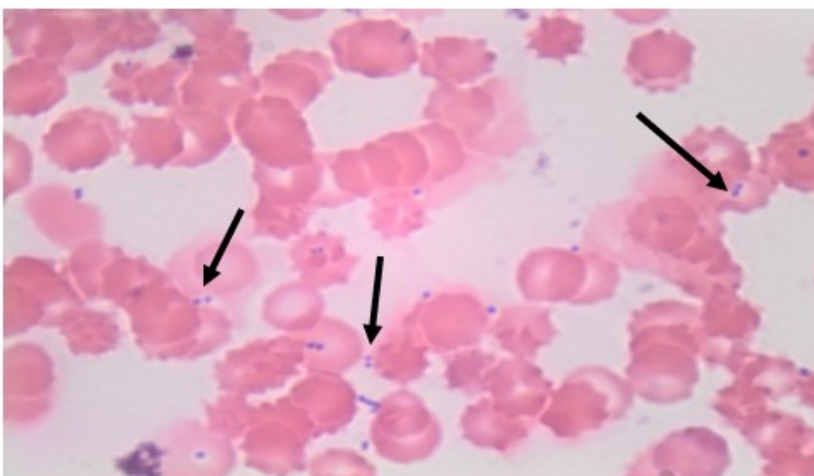


Fig. 3. Show Bipolarity of *P. multocida* stained with Leishman's staining of the heart blood of the infected mice.

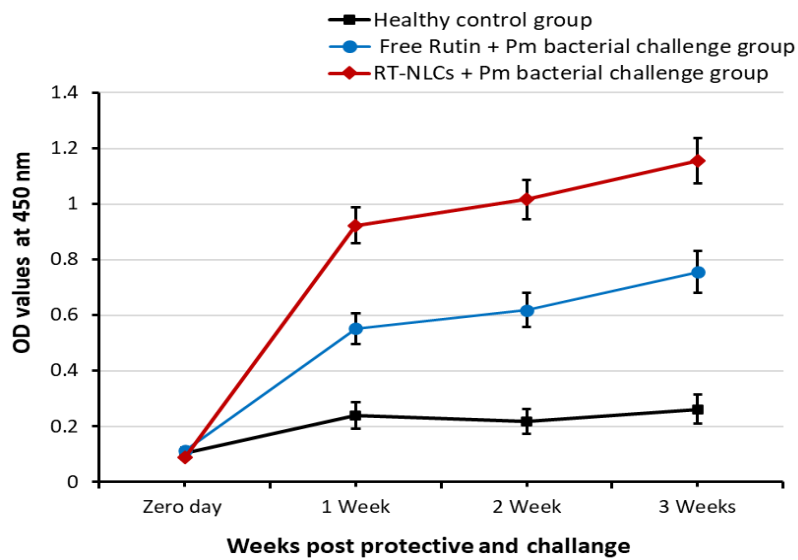


Fig. 4. Levels of IgG response measured by indirect ELISA against Rutin nanostructure lipid carrier RUT-HPMC-NLCs (◆) in protected challenged mice serum samples and Extract Free Rutin (●) before and after challenge with *P. multocida* compare with Healthy mice samples (■). Bars in the figure represent mean \pm standard deviation of the optical density.

(RUT-HPMC-NLCs): F1 Rutin nanostructure lipid carriers contain 0.1 % w/v mucoadhesive HPMC.

1-Liver

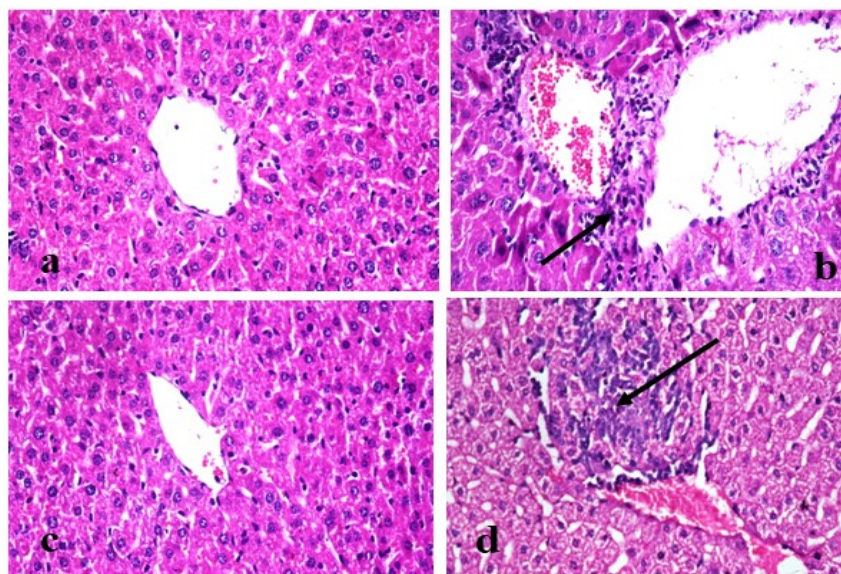


Fig. 5. I. Photomicrographs of liver from different experimental groups stained with H&E X400 showing: A; Control negative normal group 1 (0). B; Control positive group 2 with severely degenerated hepatic parenchyma, Congested hepatoportal blood vessels, and mononuclear cell infiltration (arrow) (+++). C; group 4 (protected with RUT-NLCs) with apparently healthy hepatic parenchyma (0). D; group 3 (protected with free RUT) with Moderate lesions of congested hepatoportal blood vessels and leucocytic cell infiltration (arrow) (++)

2- Lung

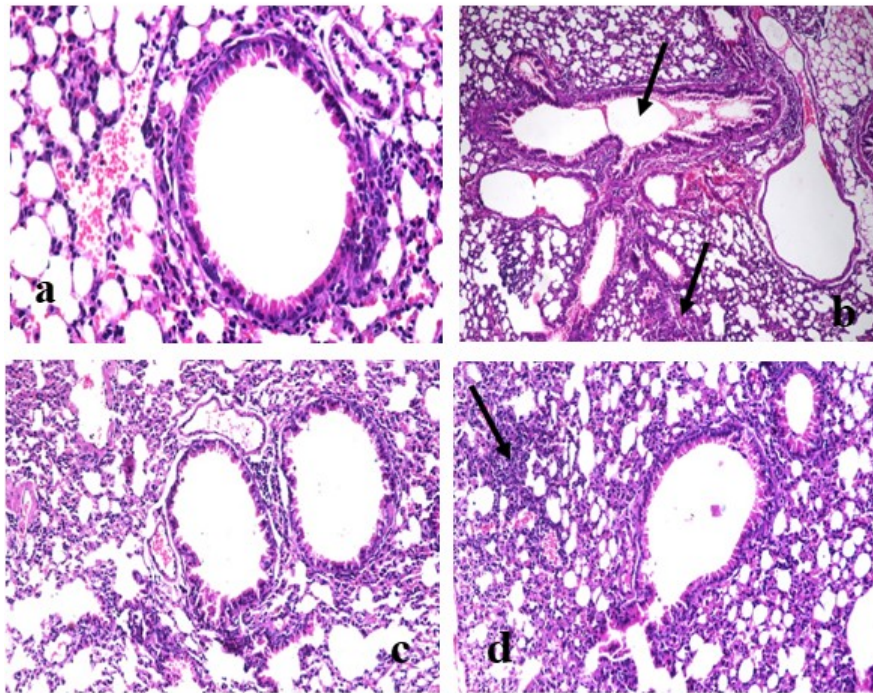


Fig. 5. II. Photomicrographs of lungs from different experimental groups stained with H&E X200 showing: A; Control negative normal group1 (0). B; Control positive group 2 with severe bronchitis (arrows) (+++). C; group 4 (protected with RUT-HPMC-NLCs) with apparently healthy pulmonary parenchyma (0). D; Group 3 (protected with free RUT) group with Moderate lesions of interstitial mononuclear cell infiltration (arrows) (++)

3- Spleen

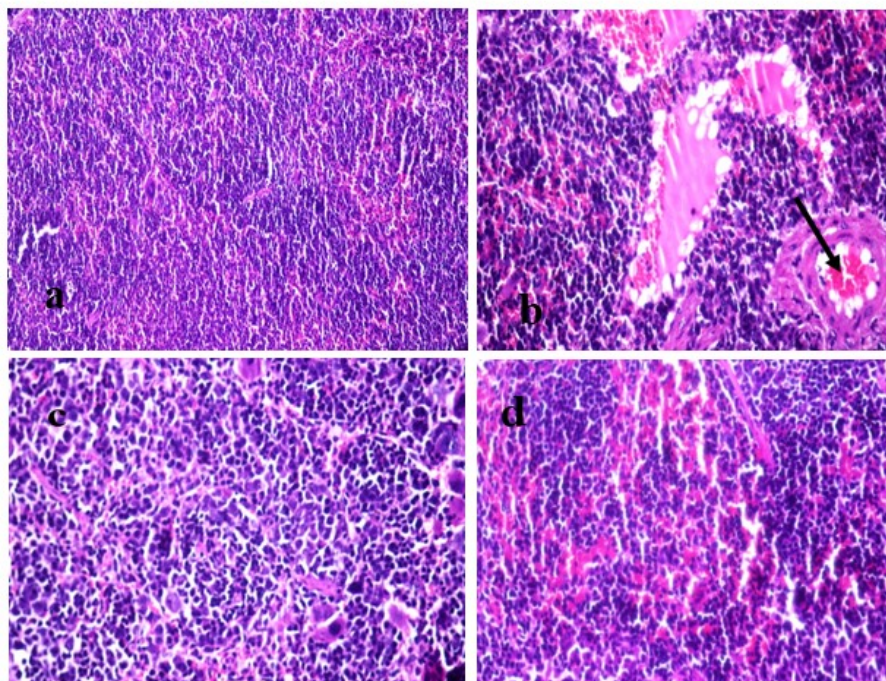


Fig. 5. III : Photomicrographs of spleens from different experimental groups stained with H&E X200 showing: A. Control negative normal group 1 (0), B. Control group 2 with severely congested red bulbs and interstitial blood vessels (arrows) (+++), C. Group 4 protected with Rutin nanostructure lipid carriers had apparently healthy splenic parenchyma (0), D. Group 3 protected with free rutin showed moderately congested red bulbs and interstitial blood vessels (++)

TABLE 1. Composition and characterisation of intranasal RUT-HPMC-NLCs mucoadhesive formulations. All measurements were performed in triplicate.

Formulations	HPMC concentration (w/v)	pH	Viscosity mPa	Homogeneity
F1	0.1	5.5± 0.04	920± 20.0	homogenous
F2	0.25	4.97± 0.05	1110± 17.0	homogenous
F3	0.5	5.5± 0.02	1250± 15.0	homogenous
F4	0.75	5.0± 0.03	1320± 13.0	homogenous

TABLE 2. Ex-vivo permeability parameters of RUT from free drug suspensions and mucoadhesive nanostructure lipid carrier formulations across nasal mucosa. (All values are presented as a mean value ± S.D of three different measurements, n=3)

Formulation	Amount permeated (µg/cm ²)	Flux (Jss) (µg/cm ² /sec)	Apparent Permeability Papp x 10 ⁻⁶ (cm/sec)	Enhancement Ratio
RUT Suspension	69.0± 24.16	2.00 ± 0.12	0.55 ±0.002	-
F1	311.64± 10.0	6.67± 0.10*#	1.85± 0.005*#	3.37
F2	250.22± 8.0	4.90 ± 0.23*	1.40±0.009*	2.55
F3	150.82± 11.5	4.26± 0.2*	1.18± 0.003*	2.15
F4	107.08± 7.4	3.047± 0.15*	0.846± 0.001*	1.54

Notes: *RUT-HPMC-NLCs significantly different compared with free drug suspension. ($p < 0.001$), # F1 (RUT-HPMC-NLCs) containing 0.1% w/v HPMC significantly different compared with other formulations (F2,F3, F4) . ($p < 0.05$)

TABLE 3. Show result of Biochemical reaction of the isolated *Pasteurella multocida* using standard laboratory tests.

Biochemical tests	Result
Indole production	+ve
Oxidase	+ve
Catalase	+ve
Urease test	-ve
MR and VP tests	-ve
TSI	+ve
Nitrate reduction	+ve
Mannitol	+ve
Lactose	-ve
Glucose	+ve
Sucrose	+ve
Arabinose	-ve
Trehalose	-ve
Mannose	+ve

Notes: +ve = positive

-ve = negative

TABLE 4 a. Illustrated the Mean ±Standard deviation of the bacterial count of *p. multocida* in the lungs

Group	Time	24h	48h	7 days
Group 1		0	0	0
Group 2		2.4 ± 0.12 (x 10 ⁷)	2.8 ± 0.12 (x 10 ⁸)	
Group 3		1.74 ± 0.1 (x 10 ⁶) *	2.56 ± 0.09 (x 10 ⁵) *	5 ± 2.64 (x 10 ²)
Group 4		2.45 ± 0.19 (x 10 ⁵) *	1.96 ± 0.1 (x 10 ³) * #	0

Data are expressed as Mean ±Standard deviation.

*Significant difference between tested groups (3 and 5) compared with infected group (2) ($p < 0.05$)

Significant difference between groups treated with optimum RUT- HPMC-NLCs compared with that treated with pure RUT. ($p < 0.05$).

(RUT-HPMC-NLCs): F1 Rutin nanostructure lipid carriers contain 0.1 % w/v mucoadhesive HPMC.

TABLE 4 b. Illustrated the as Mean ±Standard deviation of bacterial counts in the liver

Group	Time	24h	48h	7 days
Group 1		0	0	0
Group 2		2.16 ± 0.07 (x 10 ⁻⁵)	2.38 ± 0.161 (x 10 ⁻⁶)	
Group 3		2.12 ± 0.27 (x 10 ⁻⁴) *	1.13 ± 0.11 (x 10 ⁻³) *	2.33 ± 1.52 (x 10 ⁻²)
Group 4		1.14 ± 0.13 (x 10 ⁻⁴) *#	1.96 ± 0.1 (x 10 ⁻²) * #	0

Data are expressed as Mean ±Standard deviation.

*Significant difference between the tested groups (3 and 4) and infected group (2) (at p <0.05)

Significant difference between groups treated with optimum RUT- HPMC-NLCs (gr 4) and those treated with pure RUT (gr 3). (At p <0.05)

(RUT-HPMC-NLCs): F1 Rutin nanostructure lipid carriers contain 0.1 % w/v mucoadhesive HPMC.

TABLE 4 c. Illustrated the as Mean ±Standard deviation of the bacterial count in the spleen.

Group	Time	24 h	48h	7 days
Group 1		0	0	0
Group 2		1.74 ± 0.112(x10 ⁻⁸)	2.11 ± 0.146 (x10 ⁻⁹)	
Group 3		5.76 ± 1.8 (x 10 ⁻⁷) *	1.59 ± 0.16 (x10 ⁻⁵) *	2.33 ± 1.5 (x10 ⁻²)
Group 4		2.45 ± 0.10 (x 10 ⁻⁵) * #	2.34 ± 0.12 (x 10 ⁻³) * #	0

Data are expressed as Mean ±Standard deviation

*Significant difference between tested groups (3 and 4) and infected group (2) (at p <0.05) # Significant

difference between group that was protected with optimum RUT- HPMC-NLCs (gr 4) and group that was treated with pure RUT (gr 3). (At p <0.05).

(RUT-HPMC-NLCs): F1 Rutin nanostructure lipid carriers contain 0.1 % w/v mucoadhesive HPMC.

TABLE 5. Average optical density of IgG at 450 nm.

Week	Group	Healthy	Rutin-mucoadhesive nanostructure lipid carriers (RUT-HPMC-NLCs)	Free Rutin	F-Value
Zero Day		0.127 ± 0.01 ^a	0.086 ± 0.007 ^b	0.116 ± 0.005 ^c	15.83*
1 week		0.253 ± 0.004 ^c	0.923 ± 0.005 ^a	0.613 ± 0.001 ^b	8484.91**
2 weeks		0.236 ± 0.013 ^d	1.02 ± 0.005 ^a	0.693 ± 0.007 ^b	1838.21**
3 weeks		0.256 ± 0.008 ^d	1.156 ± 0.007 ^a	0.755 ± 0.006 ^c	3916.45**

Data are expressed as Mean ±Standard deviation.

*P- values < 0.05: statistically significant.

**P- values < 0.001: high statistical significance.

Means within the same row with different letters are significantly different.(RUT-HPMC-NLCs): F1 Rutin nanostructure lipid carriers contain 0.1 % w/v mucoadhesive HPMC.

TABLE 6. Summary of the immunomodulatory effects of rutin mucoadhesive nanostructure lipid carriers (RUT-HPMC-NLCs), and Free Rutin on inflammatory cytokines before and after challenge with *P. multocida* in mice compared with Healthy mice and infected mice without protected controls

Group	Parameter		Interferon Gamma (IFN- γ)	Interlukin-12	
Prophylaxis	Rutin-mucoadhesive nanostructure lipid carriers (RUT-HPMC-NLCs)	1 week	225.67 \pm 3.84 ^h	169 \pm 4.93 ^g	
		2 weeks	354.97 \pm 0.61 ^e	212.6 \pm 1.76 ^e	
		3 weeks	440 \pm 2.89 ^a	240.17 \pm 1.71 ^c	
	Free Rutin	1 week	245 \pm 2.89 ^f	186.33 \pm 3.28 ^f	
		2 weeks	420.1 \pm 1.24 ^b	232.6 \pm 1.53 ^d	
		3 weeks	402.47 \pm 1.42 ^c	259.96 \pm 0.61 ^b	
		Healthy		194.67 \pm 0.88 ^j	74.7 \pm 1.48 ^h
		Infected unprotected		370.27 \pm 0.37 ^e	270 \pm 0.64 ^a
		F-Value		2191.826**	585.895*

Data are expressed as Mean \pm Standard deviation.

*P- values < 0.05: statistically significant.

**P- values < 0.001: high statistical significance.

Means within the same column with different letters differ significantly

(RUT-HPMC-NLCs): F1 Rutin nanostructure lipid carriers contain 0.1 % w/v mucoadhesive HPMC

TABLE 7. Grading of histopathological lesions in the liver, lungs, and spleen in all groups.

	Organs	Grades of the lesions			
		0 (Negative)	+(Mild)	++ (Moderate)	+++ (Sever)
Control Negativ ^e	Liver	√			
	Lungs	√			
	Spleen	√			
Control Positiv ^e	Liver				√
	Lungs				√
	Spleen				√
Rutin nanostructure lipid carrier + PM	Liver	√			
	Lungs	√			
	Spleen	√			
Free Rutin + PM	Liver			√	
	Lungs			√	
	Spleen			√	

References

- Yang, W., Li, M., Zhang, C., Zhang, X., Guo, M. and Wu, Y., Pathogenicity, colonization, and innate immune response to *Pasteurella multocida* in rabbits. *BMC Veterinary Research*, **18**(1), 1-10(2022)
- Wu, C., Qin, X., Li, P., Pan, T., Ren, W., Li, N. and Peng, Y., Transcriptomic Analysis on Responses of Murine Lungs to *Pasteurella multocida* Infection. *Front Cell Infect Microbiol.*, **7**, 251(2017).
- Guan, L.J., Song, J.J., Xue, Y., Ai, X., Liu, Z.J., Si, L.F., Li, M.Y. and Zhao, Z.Q., Immune Protective Efficacy of China's Traditional Inactivated and Attenuated Vaccines against the Prevalent Strains of *Pasteurella multocida* in Mice. *Vaccines (Basel)*. **9**(10), 9101155(2021).
- Aldeewan, A.B., Sayhood, M.H. and Abbas, B.A., Isolation and identification of *Pasteurella multocida* from healthy and clinical cases of sheep and study their antimicrobial sensitivity. *Journal of Wassit for Science & Medicine*, **12**(1),56-67(2019).
- Zhu, D., Yuan, D., Wang, M., Jia, R., Chen, S., Liu, M., Zhao, X., Yang, Q., Wu, Y., Zhang, S., Huang, J., Liu, Y., Zhang, L., Yu, Y., Pan, L., Chen, X. and Cheng, A., Emergence of a multidrug-resistant hypervirulent *Pasteurella multocida* ST342 strain

- with a floR-carrying plasmid. *J. Glob. Antimicrob. Resist.*, **20**, 348-350(2020).
6. Bacanlı, M. and Başaran, N., Importance of antibiotic residues in animal food. *Food Chem Toxicol.*, **125**, 462-466 (2019).
 7. Deepika, M.S., Thangam, R., Vijayakumar, T.S., Sasirekha, R., Vimala, R.T.V., Sivasubramanian, S., Arun, S., Babu, M.D. and Thirumurugan, R., Antibacterial synergy between rutin and florfenicol enhances therapeutic spectrum against drug resistant *Aeromonas hydrophila*. *Microb. Pathog.*, **135**, 103612(2019).
 8. Cushnie, T.T. and Lamb, A.J., Antimicrobial activity of flavonoids. *International Journal of Antimicrobial Agents*, **26**(5), 343-356 (2005) .
 9. Vaquero, M.R., Alberto, M.R. and De Nadra, M.M., Antibacterial effect of phenolic compounds from different wines. *Food Control*, **18**(2), 93-101(2007).
 10. Rashidinejad, A., Dima, C., Karaca, A.C. and Jafari, S.M., A review on rutin-loaded nanocarriers: Fundamentals, bioavailability, application in functional foods, and challenges. *European Polymer Journal*, 113385 (2024) .
 11. Woods, A. and Rahman, K.M., Antimicrobial molecules in the lung: formulation challenges and future directions for innovation. *Future Med. Chem.*, **10**(5), 575-604 (2018) .
 12. Merlos, R., Amighi, K. and Wauthoz, N., Recent developments in inhaled triazoles against invasive pulmonary Aspergillosis. *Current Fungal Infection Reports*, **8**, 331-342 (2014) .
 13. Alexescu, T.G., Tarmure, S., Negrean, V., Cosnarovici, M., Ruta, V.M., Popovici, I., Para, I., Perne, M.G., Orasan, O.H. and Todea, D.A., Nanoparticles in the treatment of chronic lung diseases. *Journal of Mind and Medical Sciences*. **6**(2), 224-231 (2019) .
 14. Khosa, A., Reddi, S. and Saha, R.N., Nanostructured lipid carriers for site-specific drug delivery. *Biomed. Pharmacother.*, **103**, 598-613 (2018) .
 15. Varahachalam, S.P., Lahooti, B., Chamaneh, M., Bagchi, S., Chhibber, T., Morris, K., Bolanos, J.F., Kim, N.-Y., and Kaushik, A., Nanomedicine for the SARS-CoV-2: state-of-the-art and future prospects. *International Journal of Nanomedicine*, 539-560(2021).
 16. Shazwani, S.S., Marlina, A. and Misran, M., Development of Nanostructured Lipid Carrier-Loaded Flavonoid-Enriched Zingiber officinale. *ACS omega*, **9**(15), 17379-17388(2024).
 17. Muller, R.H. and Keck, C.M., Challenges and solutions for the delivery of biotech drugs--a review of drug nanocrystal technology and lipid nanoparticles. *J. Biotechnol.*, **113**(1-3), 151-170(2004)
 18. Goel, R., Mishra, R., Singh, N., Rajora, A., Singh, R. and Gaur, P.K., Nanostructured Lipid Carriers: Enhancing Herbal Medicine Delivery. *Lipid Based Nanocarriers for Drug Delivery*, 367(2024).
 19. Li, B. and Yang, X., Rutin-loaded cellulose acetate/poly (ethylene oxide) fiber membrane fabricated by electrospinning: A bioactive material. *Materials Science and Engineering: C.*, **109**, 110601(2020).
 20. Almurshedi, A.S., Aljunaidel, H.A., Alquadeib, B., Aldosari, B.N., Alfagih, I.M., Almarshidy, S.S., Eltahir, E.K. and Mohamoud, A.Z., Development of inhalable nanostructured lipid carriers for ciprofloxacin for noncystic fibrosis bronchiectasis treatment. *International Journal of Nanomedicine*, 2405-2417(2021).
 21. Patil, A.G. and Jobanputra, A.H., Rutin-chitosan nanoparticles: fabrication, characterization and application in dental disorders. *Polymer-Plastics Technology and Engineering*, **54**(2), 202-208(2015).
 22. Mohamed, A.M., Toaleb, N.I., Allam, A.M., Hekal, S.H.A., Abdelgayed, S.S. and Hassan, A.S., Preparation and Characterization of Alginate Nanocarriers as Mucoadhesive Intranasal Delivery Systems for Ameliorating Antibacterial Effect of Rutin Against *Pasteurella Multocida* Infection in Mice. *OpenNano*, 100176(2023).
 23. Songer, J.G.a.P., K.W. , *Veterinary Microbiology: Bacterial and Fungal Agents of Animal Disease*. Vol. ISBN: 9780721687179, . 2005, USA: Elsevier Saunders.
 24. El Fakhry, Y., Achbarou, A., Desportes-Livage, I. and Mazier, D., Encephalitozoon intestinalis: Humoral responses in interferon- γ receptor knockout mice infected with a microsporidium pathogenic in AIDS patients. *Experimental Parasitology*, **89**(1), 113-121(1998).
 25. Praveena, P.E., Periasamy, S., Kumar, A. and Singh, N., Cytokine profiles, apoptosis and pathology of experimental *Pasteurella multocida* serotype A1 infection in mice. *Research in Veterinary Science*, **89**(3), 332-339(2010).
 26. Meinhart, A.D., Damin, F.M., Caldeirao, L., Teixeira-Filho, J. and Godoy, H.T., Rutin in herbs and infusions: screening of new sources and consumption estimation. *Food Science and Technology*, **40**, 113-120(2020).
 27. Verekar, R.R., Gurav, S.S. and Bolmal, U., Thermosensitive mucoadhesive in situ gel for intranasal delivery of Almotriptan malate: Formulation, characterization, and evaluation. *Journal of Drug Delivery Science and Technology*. **58**, 101778(2020).
 28. Galgatte, U.C., Kumbhar, A.B. and Chaudhari, P.D., Development of in situ gel for nasal delivery: design, optimization, in vitro and in vivo evaluation. *Drug delivery*, **21**(1), 62-73(2014).
 29. Rezaie, A., Gharibi, D., Ghorbanpoor, M., Anbari, S. and Pourmahdi Broojeni, M., Evaluation of immunopathologic effects of aqueous extract of *Echinacea purpurea* in mice after experimental challenge with *Pasteurella multocida* serotype A. *Iran. J. Vet. Res.*, **15**(4), 379-384(2014).
 30. Lowry, O.H., Rosebrough, N.J., Farr, A.L. and Randall, R.J., Protein measurement with the Folin

- phenol reagent. *J. Biol. Chem.*, **193**(1), 265-275(1951).
31. Engvall, E. and Perlmann, P., Enzyme-linked immunosorbent assay (ELISA). Quantitative assay of immunoglobulin G. *Immunochemistry*, **8**(9), 871-874(1971).
32. Hillyer, G.V., Soler de Galanes, M., Rodriguez-Perez, J., Bjorland, J., Silva de Lagrava, M., Ramirez Guzman, S. and Bryan, R.T., Use of the Falcon assay screening test--enzyme-linked immunosorbent assay (FAST-ELISA) and the enzyme-linked immunoelectrotransfer blot (EITB) to determine the prevalence of human fascioliasis in the Bolivian Altiplano. *Am. J. Trop. Med. Hyg.*, **46**(5), 603-609(1992).
33. Bancroft, D.; Stevens, A.a.T., R. , Theory and practice of histologic technique Vol. 4th end. 2010: Churchill Livingstone.
34. Arsad, S., Esa, N. and Hamzah, H., Histopathologic changes in liver and kidney tissues from male Sprague Dawley rats treated with *Rhaphidophora decursiva* (Roxb.) Schott extract. *J. Cytol. Histol. S.*, **4**(1), 1-6(2014).
35. Snedecor, G.W.a.C., W.G. , Statistical Methods. Vol. 7th Edition. 1980: Iowa State University Press, Ames.
36. Serra, L., Doménech, J. and Peppas, N.A., Engineering design and molecular dynamics of mucoadhesive drug delivery systems as targeting agents. *European Journal of Pharmaceutics and Biopharmaceutics*, **71**(3), 519-528(2009).
37. Wang, Y., Li, M., Qian, S., Zhang, Q., Zhou, L., Zuo, Z., Lee, B., Toh, M. and Ho, T., Zolpidem Mucoadhesive Formulations for Intranasal Delivery: Characterization, In Vitro Permeability, Pharmacokinetics, and Nasal Ciliotoxicity in Rats. *J. Pharm. Sci.*, **105**(9), 2840-2847(2016).
38. Contri, R., Fiel, L., Alnasif, N., Pohlmann, A., Guterres, S. and Schäfer-Korting, M., Skin penetration and dermal tolerability of acrylic nanocapsules: Influence of the surface charge and a chitosan gel used as vehicle. *International Journal of Pharmaceutics*, **507**(1-2), 12-20(2016).
39. Pathak, R., Dash, R.P., Misra, M. and Nivsarkar, M., Role of mucoadhesive polymers in enhancing delivery of nimodipine microemulsion to brain via intranasal route. *Acta Pharmaceutica Sinica B.*, **4**(2), 151-160.(2014).
40. Praveena, P.E., Periasamy, S., Kumar, A.A. and Singh, N., Cytokine profiles, apoptosis and pathology of experimental *Pasteurella multocida* serotype A1 infection in mice. *Res. Vet. Sci.*, **89**(3), 332-339(2010).
41. Pors, S.E., Chadfield, M.S., Sørensen, D.B., Offenberg, H., Heegaard, P.M., Bisgaard, M. and Jensen, H.E., Pathology, tissue metalloproteinase transcription and haptoglobin responses in mice after experimental challenge with different isolates of *Pasteurella multocida* obtained from cases of porcine pneumonia. *J. Comp. Pathol.*, **145**(2-3), 251-260 (2011).
42. Popescu, R., Ghica, M.V., Dinu-Pîrvu, C.E., Anuța, V., Lupuliasa, D. and Popa, L., New Opportunity to Formulate Intranasal Vaccines and Drug Delivery Systems Based on Chitosan. *Int. J. Mol. Sci.*, **21**(14),5016(2020).
43. Negahdari, R., Bohlouli, S., Sharifi, S., Maleki Dizaj, S., Rahbar Saadat, Y., Khezri, K., Jafari, S., Ahmadian, E., Gorbani Jahandizi, N. and Raeesi, S., Therapeutic benefits of rutin and its nanoformulations. *Phytother. Res.*, **35**(4), 1719-1738(2021).
44. Luo, M., Sui, Y., Tian, R. and Lu, N., Formation of a bovine serum albumin diligand complex with rutin for the suppression of heme toxicity. *Biophys Chem.*, **258**, 106327(2020).
45. Bretkopf, D.M., Jankowski, V., Ohl, K., Hermann, J., Hermert, D., Tenbrock, K., Liu, X., Martin, I.V., Wang, J., Groll, F., Gröne, E., Floege, J., Ostendorf, T., Rauen, T. and Raffetseder, U., The YB-1:Notch-3 axis modulates immune cell responses and organ damage in systemic lupus erythematosus. *Kidney Int.*, **97**(2), 289-303(2020).
46. Wang, T., Miao, M., Bai, M., Li, Y., Li, M., Li, C. and Xu, Y., Effect of sophora japonica total flavonoids on pancreas, kidney tissue morphology of streptozotocin-induced diabetic mice model. *Saudi J. Biol. Sci.*, **24**(3), 741-747(2017).
47. Trinchieri, G., Interleukin-12 and the regulation of innate resistance and adaptive immunity. *Nat. Rev. Immunol.*, **3**(2), 133-46.(2003)
48. Happel, K.I., Dubin, P.J., Zheng, M., Ghilardi, N., Lockhart, C., Quinton, L.J., Odden, A.R., Shellito, J.E., Bagby, G.J., Nelson, S. and Kolls, J.K., Divergent roles of IL-23 and IL-12 in host defense against *Klebsiella pneumoniae*. *J. Exp. Med.*, **202**(6), 761-769(2005).
49. Nguyen, T.A., Liu, B., Zhao, J., Thomas, D.S. and Hook, J.M., An investigation into the supramolecular structure, solubility, stability and antioxidant activity of rutin/cyclodextrin inclusion complex. *Food Chem.*, **136**(1), 186-192(2013).

تقييم التأثير الوقائي للروتين باستخدام الجسيمات النانومترية نظام الأنفية الداخلية المتقدمة في الفئران كنموذج بعد إصابتها بالعدوى تجريبياً بالبكتريا الباستوريلا مولتوسيدا المعزولة من الأغنام المصابة طبيعياً

إيمان عبد الرحيم محمود¹، أماني محمد محمد محمد²، نجوى إبراهيم تعيلب²، أحمد محمد علام²، شيرين سعيد عبد الجيد³، عبير سعد حسن⁵ وسحر حسين عبد الله هيك⁶

¹ قسم العقاقير، كلية الصيدلة، جامعة جنوب الوادي قنا، مصر.

² قسم الطفيليات وأمراض الحيوان، معهد البحوث البيطرية، المركز القومي للبحوث، 33 شارع البحوث، الدقي، 12622 الجيزة، مصر.

³ قسم الباثولوجي، كلية الطب البيطري، جامعة توسكيجي، الولايات المتحدة الأمريكية.

⁴ قسم الباثولوجي، كلية الطب البيطري، جامعة القاهرة، 12211، الجيزة، مصر.

⁵ قسم الصيدلانيات، كلية الصيدلة، جامعة جنوب الوادي، قنا 83523، مصر.

⁶ قسم الموارد الطبيعية، كلية الدراسات الأفريقية العليا، جامعة القاهرة، الجيزة، مصر.

الخلاصة

الروتين هو مكمل غذائي واعد له أنشطة مضادة للبكتيريا ووقائية محتملة. يهدف هذا العمل إلى تقييم التأثير الوقائي لمركب الروتين النانومتري، والذي تم تصنيعه كمتحضر لاصق مخاطي يتم تناوله عن طريق الأنف، على الفئران التي تم اختيارها تجريبياً وإصابتها بالعدوى البكتيرية الباستوريلا مولتوسيدا. وقد تم تحميل مستخلص الروتين بالنانو في تركيزات مختلفة من هيدروكسي بروبيل ميثيل السليلوز (HPMC) اللصق للمخاط. وتم تقييم نفاذية تركيبات روتين النانومترية خارج الجسم الحي عبر الغشاء المخاطي للأنف. تم فحص التركيبة المثلى في الجسم الحي، ولم تكن المجموعة 1 مصابة أو محصنة. أما المجموعة 2 مصابة بالبكتيريا الباستوريلا مولتوسيدا وغير محصنة، وكانت المجموعتان 3 و4 عبارة عن مجموعات محصنة بمستخلص روتين الحر ومستخلص روتين النانومترية على التوالي، عن طريق التقطير أو التنقيط بالأنف. تم إجراء العد البكتيري في جميع الأعضاء الحيوية بعد العدوى بالبكتريا لمعرفة مدى التأثير الوقائي لمستخلص الروتين الحر والمحمل بالنانو، كما تم عمل الباثولوجي لتحديد التغيرات المرضية للأنسجة. تم تحديد مستوى IgG، وتركيز السيتوكينات، وتم تقييم إنترفيرون جاما (IFN- γ) وإنترلوكين-12 (IL-12) باستخدام ELISA ساندويتش. وقد أظهرت النتائج أن نظام مستخلص الروتين المحمل بجزيئات النانو والذي يحتوي على أقل كمية من HPMC كمية نفاذة معززة (10.0 ± 311.64 ميكروجرام / سم 2) وتدفق ثابت 0.10 ± 6.67 ميكروجرام / سم 2 / ثانية عبر الغشاء المخاطي للأنف وقد لوحظ انخفاضاً كبيراً في عدد البكتيريا، ولم تظهر تغيرات في أنسجة الأعضاء المفحوصة باثولوجياً. وأيضاً قد أثر على تعديل الاستجابة المناعية الخلوية والخلوية للفئران حيث زاد من مستويات الأجسام المضادة IgG، وكانت مستويات تركيز الإنترفيرون جاما أعلى بشكل ملحوظ (قيم $P < 0.001$)، وكانت قيم تركيز والإنترلوكين 12 أيضاً أعلى بشكل ملحوظ (قيم $P < 0.05$) في مجموعة الفئران 4 مقارنة بالفئران التي تم تطعيمها عن طريق الأنف باستخدام الروتين الحر (المجموعة 3). الاستنتاج: قد توصلنا في هذه الدراسة إن المادة النانوية التي يتم لصقها داخل الأنف باستخدام الروتين لها تأثيرات مناعية ملحوظة ويمكن استخدامها للحماية ضد الباستوريلا مولتوسيدا في الحيوانات.

الكلمات الدالة: الباستوريلا مولتوسيدا، الوقاية، مستخلص الروتين، جزيئات مستخلص الروتين النانومترية.